Mon. Not. R. Astron. Soc. **000**, 000–000 (0000) Printed 23 January 2021 (MN LATEX style file v2.2)

CK Vul: evolving nebula and three curious background stars

M. Hajduk,[1] P.A.M. van Hoof,[2] A.A. Zijlstra[3]
[1] *Nicolaus Copernicus Astronomical Center, ul. Rabiańska 8, 87-100 Toruń, Poland*
[2] *Royal Observatory of Belgium, Ringlaan 3, 1180 Brussels, Belgium*
[3] *Jodrell Bank Centre for Astrophysics, Alan Turing Building, Manchester M13 9PL, UK*

ABSTRACT

We analyse the remnants of CK Vul (Nova Vul 1670) using optical imaging and spectroscopy. The imaging, obtained between 1991 and 2010, spans 5.6% of the lifetime of the nebula. The flux of the nebula decreased during the last 2 decades. The central source still maintains the ionization of the innermost part of the nebula, but recombination proceeds in more distant parts of the nebula. Surprisingly, we discovered two stars located within 10″ of the expansion centre of the radio emission that are characterized by pronounced long term variations and one star with high proper motion. The high proper motion star is a foreground object, and the two variable stars are background objects. The photometric variations of two variables are induced by a dusty cloud ejected by CK Vul and passing through the line of sight to those stars. The cloud leaves strong lithium absorption in the spectra of the stars. We discuss the nature of the object in terms of recent observations.

Key words: stars: AGB and post-AGB–binaries: general – stars: evolution – stars: individual: CK Vul – stars: mass-loss – planetary nebulae: general

1 INTRODUCTION

CK Vul erupted in 1670, becoming a 2.6 magnitude star at its maximum (Shara & Moffat 1982). With its two subsequent fadings and recoveries on the timescale of one year, the 1670-72 lightcurve remains very intriguing as well as poorly understood. The object was interpreted as a slow nova (Shara et al. 1985), born-again star (Harrison 1996; Evans et al. 2002), or finally, a stellar merger (Kato 2003). Recently, Miller Bertolami et al. (2011) proposed the diffusion-induced nova scenario for CK Vul.

The central star has not been observed since its decline in 1672 (Naylor et al. 1992), leaving us with no chance to inspect the product of the outburst directly. The current limit for the central object brightness is $r' > 23$ mag (Hajduk et al. 2007). The apparent amplitude of the outburst may have possibly been as large as 20 mag or more.

What we currently observe is a gaseous nebula with a maximum extent of the symmetric, limb-brightened lobes of about 1′. The expansion measurements have proven that it indeed dates back to the XVII century (Hajduk et al. 2007). Different parts of the nebula show enhanced [NII] lines exceeding in intensity the Hα emission. A faint, barely resolved radio emission is detected at the centre of expansion.

We have discovered two variable stars located within $3-4$ arcsec of the expansion centre in the plane of the sky. The apparent separation of the two variable stars is about 2 arcsec. The coincidence of the position of the stars with the expansion centre of the CK Vul nebula is striking. In addition, we found a star with pronounced proper motion in the vicinity of the expansion center of CK Vul. In this paper, we investigate the link of the variable and high proper motion star with CKVul and discuss the nature of the object in the light of new observations.

2 OBSERVATIONS AND DATA REDUCTION

CK Vul was observed with the WHT telescope with the Prime Focus Camera. The service programme observations were carried in the R and Hα 6559/57 filters on April 14th, 2009.

Imaging was also performed on the Gemini Multi-Object Spectrograph (GMOS) at three different epochs in 2010 with the Sloan $g'r'i'z'$ wide band filters and on one occasion with various emission lines and corresponding continuum filters (Table 1). The transformation equations between the $UBVR_CI_C$ and $g'r'i'z'$ systems were provided by Smith et al. (2002).

The data were reduced using the IRAF GMOS pack-

Table 1. A log of the CK Vul imaging observations. The data were taken with the 4.2-m William Herschel Telescope (WHT), the 2.54-m Isaac Newton Telescope (INT) and the 8.1-m Gemini North (GN).

date	telescope	filters used
1991-08-10	WHT	Hα R
2004-09-04	INT	Hα r'
2005-07-12	INT	Hα $r'i'$
2009-04-14	WHT	Hα R
2010-04-23	GN	$g'r'i'z'$
2010-06-10	GN	$g'r'i'z'$
2010-06-22	GN	Hα [O III] [S II] redshifted Hα redshifted [O III]
2010-06-23	GN	$g'r'i'z'$

age. The instrumental magnitudes were derived using the IRAF DAOPHOT package. The absolute flux calibration for the photometry was obtained using the 2010 April 23 observation of the SA 110-361 Landolt standard field and the 2010 June 23 observation of the PG 2213-006 field and the standard Mauna Kea extinction curve. Six standard stars were present in the SA 110-361 field and four in the PG 2213-006 field. The rms of the fit for the SA 110-361 (PG 2213-006) field was 0.12 (0.06), 0.08 (0.05), 0.06 (0.02) and 0.06 (0.03) mag for the g', r', i' and z' filters, respectively.

The magnitudes for the remaining archive images (either in the Sloan or Johnson-Morgan-Cousins system) were calibrated with respect to the 2010 June 23 and April 23 observations using all the available field stars, by means of a least squares linear fit.

The r' and i' magnitudes derived from the GMOS imaging were checked against the IPHAS catalogue (Drew et al. 2005). For this purpose, IPHAS magnitudes were converted from the Vega to the AB_{95} system (Fukugita et al. 1995). The IPHAS and GMOS absolute calibration agree to about 0.08 magnitude in r' and 0.02 magnitude in i'.

Emission line images in the Hα, [O III] and [S II] bands were continuum subtracted using redshifted Hα (for Hα and [S II]) and [O III] filters using the ISIS package, accounting for different PSFs (Alard & Lupton 1998).

Longslit spectra at seven different positions were taken with the GEMINI North GMOS facility on June 10th, 12th and 14th, 2010. The slit positions are plotted in Figure 1. In four positions the slit was centered on the nebula, including the three brightest nebulosities near the center and the tips of the bipolar nebula. Three other observations were centered on the field stars. Only the slit positions centered on the nebula are numbered in Figure 1.

The B600 grating was used and the central wavelength was set at 550 or 560 nm. The spectra were calibrated using a spectrophotometric standard star BD+25 3941 observed during spectroscopic nights. The mean extinction curve at Mauna Kea was used. The reduction was performed using the IRAF GMOS package.

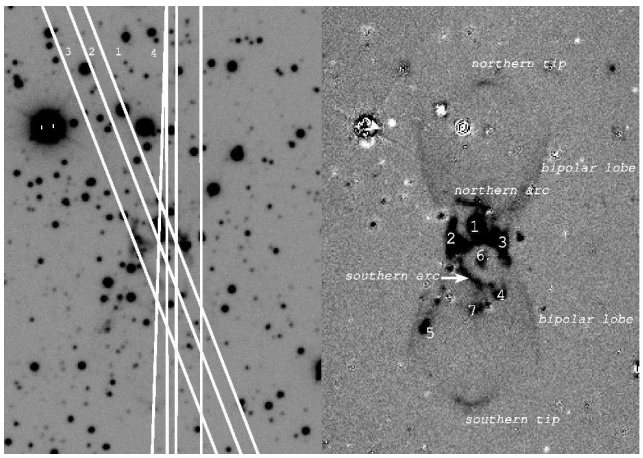

Figure 1. The positions of the slit for the spectroscopic observations on the background of the GMOS mosaic Hα image (left). The slit width was wider than indicated in the figure. Four out of seven slit positions are numbered. The Hα continuum subtracted image is shown on the right. The nebular components are named or numbered as in Hajduk et al. (2007). North is at the top, East to the left. The image scale is 100 × 80 arcsec.

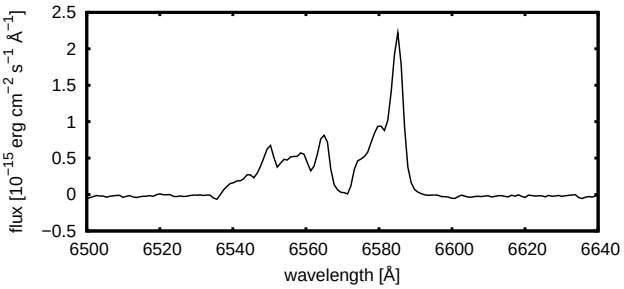

Figure 2. Spectrum of the southern part of blob 1 showing the Hα and [N II] lines.

3 THE CENTRAL STAR AND THE NEBULA OF CK VUL

3.1 Morphology and kinematics of the nebula

The central region of the nebula consists of a group of individual blobs and arcs (Figure 1). Three brightest blobs (1, 2 and 3) are accompanied by smaller blobs and arcs. All these components are embedded in a faint, limb-brightened bipolar nebula resembling an hourglass. Two tips located on the symmetric axis are the furthermost structures of the bipolar nebula.

The spectrum taken at the 1st position was centered on blob 3. Blob 3 can be decomposed into two parts characterized by different radial velocities. The southern part of the blob shows a radial velocity gradient along the slit. The northern part of blob 3 is blue-shifted with respect to the southern part. Other fainter parts of the nebula showing different velocities are observed north of the brightest parts of blob 3. The slit cuts through the northern arc in this position. The extended, faint emission seen only in the Hα and [N II] lines originates in the western edge of the southern lobe.

The second slit includes blobs 1, 6, 4 and the northern

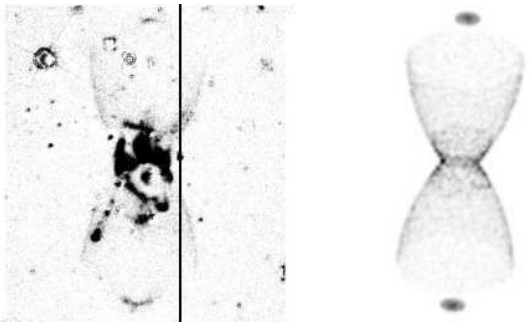

Figure 3. The Hα image (left) and the model (right) of the bipolar nebula of CK Vul. Both images are 80×70 arcsec. North is at the top, East to the left. The vertical line marks the position of the slit.

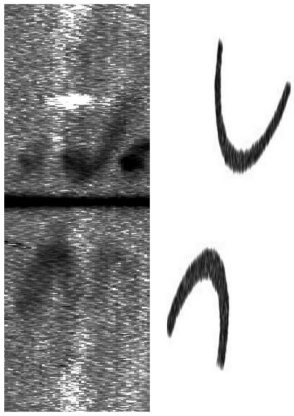

Figure 4. The modelled and observed resolved spectrum of the bipolar nebula. The stellar trace of the fast star is in the centre. The spectral coverage is about 60Å, centered at the wavelength of 6580Å. The spatial extent is about 80 arcsec.

arc. A blue-shifted, separate velocity component is seen in the southern part of nebulosity 1. It is indistinguishable from nebulosity 1 in the image (Figure 2).

The third slit cuts through the nebulosity 2, the southern arc and blob 7. The faint edge of the northern lobe is seen above blob 2, showing a positive radial velocity, increasing with the distance from the center of the nebula, and Hα stronger than the [N II] 6584 Å line.

Nebulosity 2 is not a part of the bipolar nebula since it shows different velocity gradient along the slit and negative (with respect to the systemic velocity) velocities, while northern lobe of the bipolar nebula shows positive velocities. Blob 2 is not limb-brightened, contrary to the bipolar nebula.

The fourth slit includes the tips of the bipolar nebula and blob 1. In the southern part of blob 1, near the centre of the nebula, an additional, faint component is seen at negative velocities. The same component is observed in the second slit. The radial velocity of blob 1 decreases with the distance from the center of the nebula. This suggests that blob 1 lies in the plane perpendicular to the symmetric axis of the bipolar nebula.

The three remaining spectra, obtained at the PA of 0 degree, were centered on the two variable stars and the high proper motion star.

We used the SHAPE tool (Steffen et al. 2010) in order to reproduce the structure of the bipolar nebula. We used the Hα nebular image (Figure 3) and the spectrum taken at the position of the fast star (Figure 4). The slit covered a relatively bright part of the bipolar nebula, unaffected by the bright, central nebula. An inclination angle of 65 degrees was obtained. The modelled and observed image and spectrum of the bipolar nebula are shown in Figure 3 and 4. The obtained expansion distance of (0.70 ± 0.15) kpc is in agreement with the extinction distance from Shara et al. (1985). The expansion velocity of the bipolar tips, which are the fastest components of the nebula, is about $900\,\mathrm{km\,s^{-1}}$.

3.2 The brightness drop of the nebula

We used the ISIS subtraction package (Alard & Lupton 1998) in order to investigate the motion and a possible brightess change of the nebula. We have chosen the 1991 and 2009 WHT images for the analysis, since those used a similar Hα filter. Both images were spatially aligned and the intensity scale was matched using the background stars. The PSF of the 1991 image was matched to the PSF of the 2009 image. Then the background stars were removed. The convolved 1991 and the 2009 image are shown in Figures 5a and b.

In the next step, the 2009 image was subtracted from the 1991 image. As expected, a strong residual pattern due to the nebular expansion between 1991 and 2009 was left (Figure 5c). In order to compensate for the nebular expansion, we magnified the 1991 image by a factor of 1.053, corresponding to the linear expansion of the nebula since 1670, prior to the subtraction. It reduced the residual pattern caused by the nebular expansion. However, a residual emission near the center of expansion remained in the new differential image (Figure 5d). It can be attributed to a decrease of the flux of the Hα and [N II] lines. The southernmost part of the brightest blob 1 appears to have remained unchanged, but in the north-eastern part the flux has dropped significantly between 1991 and 2009. Other parts of the nebula are also affected by the flux change.

Finally, we checked if this differential pattern could be caused by proper motion of the nebula with respect to the background stars. We matched the intensity of the nebula in the 2009 and magnified 1991 images prior to the subtraction for clarity. The differential image confirms that the flux did not drop uniformly in the nebula, affecting mostly the north-eastern part of the blob 1, and blobs 4 and 5 (Figure 5e). The south-western part of the blob 1 is unaffected by the brightness change. The gradient of the brightness change is parallel to the longest extent of blob 1. The observed differential pattern could result from the proper motion of the nebula aligned with the longest extent of blob 1. In order to examine this possibility, we shifted the 1991 image along the longest extent of blob 1, by 1.0 pix south and 0.5 pix west prior to the subtraction. In the result, the peak of the residual emission moved to the center of blob 1 (Figure 5f). Negative residuals remained in the south and appeared in the north-eastern part of the blob 1. Thus, proper motion cannot account for the differential pattern seen in the residual image.

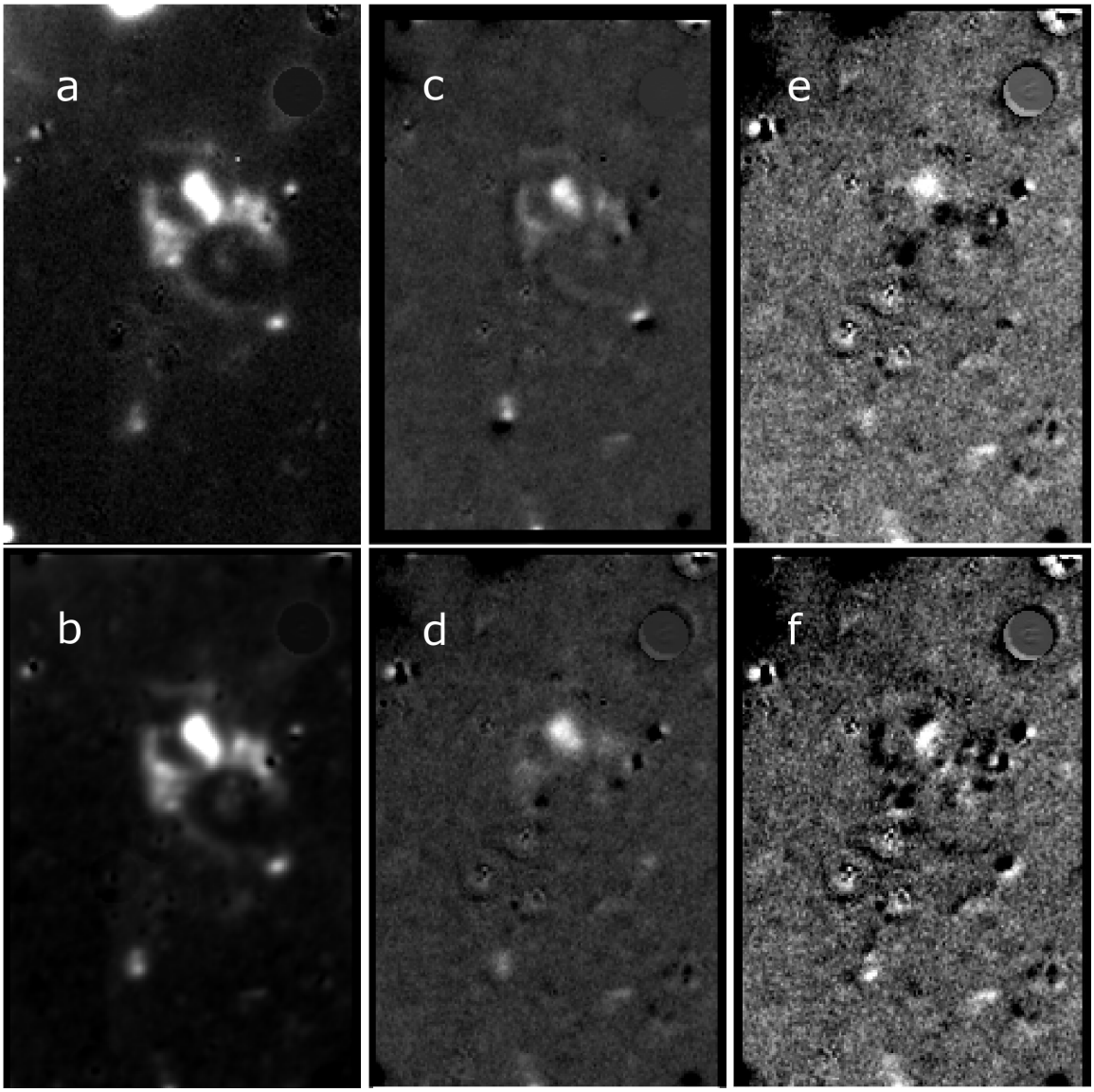

Figure 5. Hα+[N II] image of the central (40×60 arcsec) region of the nebula made in 2009 and 1991 (a and b, respectively), 1991 minus 2009 and magnified 1991 minus 2009 (c and d), re-scaled Hα+[N II] 1991 image minus 2009 and shifted 1991 minus 2009 (e and f). A star in the upper right corner was used as a PSF model. North is at the top, East to the left.

3.3 Line ratios

We examined the Hα/[N II] 6584Å line ratio in the nebula. There are no regions where Hα remained undetected, indicating lack of H-poor material in the nebula of CK Vul. The Hα/[N II] 6584Å line ratio ranges from 0.3 to 1, except at the edge of the bipolar nebula, where it is higher. The Hα line exceeds in intensity the [N II] 6584Å line only in the bipolar lobes.

Diagnostic lines of [S II] and [N II] were observed in the nebula. The density derived from the [S II] 6716/6731 Å line ratio indicates an electron density of 600 cm^{-3} for blobs 1, 2 and 4. The derived electron density in the tips of the bipolar nebula is 200 cm^{-3}. The electron temperature derived from the [N II] 5755Å to the [N II] 6548Å + 6584Å line ratio is 12 000 K for blob 1 (Table 2).

We determined an interstellar reddening of $E(B-V) = 0.7$, using the observed Balmer decrement and adopting the

Table 2. Dereddened and modelled (for $\log T_{\rm eff}$ [K] = 4.75 and 5) line intensities in selected parts of the CK Vul nebula (relative to Hβ = 100).

λ_0 [Å]	ion	blob 1	n. tip	$\log T_{\rm eff} = 4.75$	$\log T_{\rm eff} = 5$
4959	[O III]	94		38	121
5007	[O III]	280		115	364
5200	[N I]	69		6	17
5755	[N II]	14		4	8
5876	He I	31		15	15
6300	[O I]	26		25	69
6363	[O I]	10		8	22
6548	[N II]	218	129		
6563	Hα	283	283	294	292
6584	[N II]	656	403	438	644
6716	[S II]	78	90	62	109
6731	[S II]	76	59	69	114

total to selective extinction ratio $R_V = 3.1$. For the spectra made on June 14th, the derived reddening is much higher ($E(B-V) = 1.05$). The synthetic magnitudes of the objects derived on that night do not agree with the photometry. The sensitivity curve on that night differs from the sensitivity curves derived on the two other nights. An uncertain calibration of the spectrum could result from changing weather conditions between the standard star and target observations. The value of $E(B-V) = 0.7$ obtained on the June 12th is similar to the reddening given by Shara et al. (1985).

The observed drop of the nebular flux may be ascribed to the slowly proceeding recombination of hydrogen and nitrogen. The timescale of the recombination of H^+ to H^0 is 127 years for a density of $600\,\mathrm{cm}^{-3}$ (Nahar & Pradhan 1997). The timescale of the recombination of N^+ to N^0 is about 100 years at the same density. We observe a drop in the flux by about 20-30% between 1991 and 2009. If there was no ionizing radiation, the flux would drop only by 15% during that period, if charge transfer was not taken into consideration. Charge transfer between the N^+ and H^0 becomes important in a partly neutral medium. It may effectively shorten the timescale of recombination N^+ to N^0.

At very low densities the recombination timescale for hydrogen may be of the order of a thousand years. Doubly ionized nitrogen may have had not enough time to recombine and charge transfer is not yet important. This could result in an enhanced H to [N II] line ratio observed in the bipolar lobes.

The central source appears to be still active and to maintain the ionization of the innermost parts of the nebula, in particular the southern part of nebulosity 1, not affected by the brightness drop. The [O III] 5007Å emission is concentrated near the presumed position of the central source (Figure 6). The recombination timescale for $O^{++} \rightarrow O^+$ at $n_e = 600$ is only 21 years, ignoring charge transfer (Nahar & Pradhan 1997). An O^{++} sphere of the radius of 3×10^{16} cm (about 3 arcsec at the distance to CK Vul) would require continuous ionization by the central source, e.g. characterized with $L \approx 3L_\odot$ and $T_\star = 60000$ K. Radio observations confirm, that the central source is still active, although its luminosity may be gradually decreasing (Hajduk et al. 2007).

We run CLOUDY models in order to reproduce the line intensity ratios in the innermost part of the nebula (which does not show flux change in time). Table 2 presents line ratios obtained for the model.

We computed the ionized mass using the image and spectra. We approximated the 1st blob with a filled cylinder of 6 arcsec height, 1.5 arcsec radius and the mean proton density of $600\,\mathrm{cm}^{-3}$, and the 2nd and 3rd blobs with filled cones with densities of 300 and $600\,\mathrm{cm}^{-3}$ and radius and height of 5 and 6.5 arcsec, respectively. The total ionized mass of the central nebula is about $6\times10^{-5}M_\odot$. The mass of the limb-brightened bipolar nebula may be one order of magnitude higher. This is two orders of magnitude less than the mass of the nebula estimated in Hajduk et al. (2007), who assumed uniform nebular density throughout the bipolar nebula.

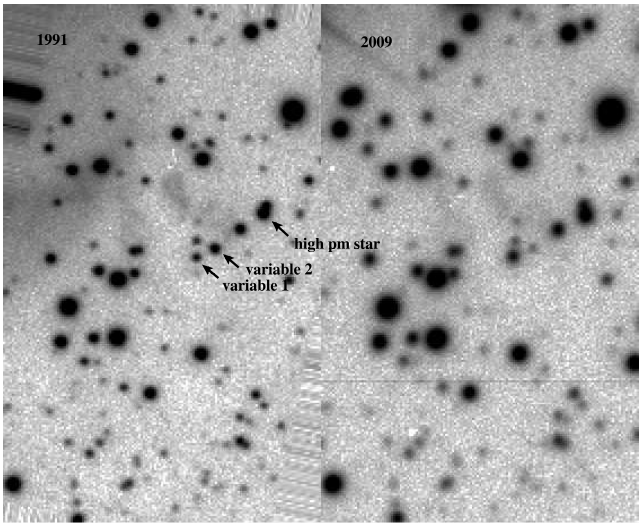

Figure 7. Comparison of the 1991 and 2009 R band images. The high proper motion and two variable stars are marked with arrows. North is at the top, East to the left. The image scale is 60×40 arcsec.

4 THE FAST STAR IN THE VICINITY OF CK VUL

4.1 Proper motion of the star and the nebula

The R band images taken in 1991 and 2009 are presented in Figure 7. One of the stars in the vicinity of CK Vul is characterized by high proper motion. The direction of the motion of the star appears to point away from the center of the nebula. We attempted to verify a possible link of the high proper motion star with CK Vul.

The Gemini image of CK Vul taken through the Hα filter is presented in Figure 8. We fitted stellar positions in the 2010 and 1991 images using the IRAF DAOPHOT package. Arrows mark extrapolated proper motions of the stars between 1670 and 2010. The mean proper motion of all the field stars present in both images (excluding the three stars for which association with CK Vul is investigated), serves as the reference frame.

In addition, we measured the proper motions of blob 4 and 5. They are marked in Figure 8 along with the error bars. We measured the centroid positions, since both of the blobs are extended and cannot be fitted with a stellar PSF. The proper motions measured for the nebular blobs are less accurate than for stars. The error bars are derived from the rms of the centroid positions measured using different radii.

The high proper motion star is characterized by $\mu = 1000\,\mathrm{mas\,yr}^{-1}$ at a position angle of 244.4 degree (or $\mu_\alpha = -900\,\mathrm{mas\,yr}^{-1}$ and $\mu_\delta = -400\,\mathrm{mas\,yr}^{-1}$). The extrapolated position of the fast star is a few arcseconds north of the position of the nebula determined for 1670, when the outburst occured. The accuracy of the position determination of the star on both images may be questioned due to blending with a nearby field star. However, the PSF fitting algorithm was able to resolve both stars. The residuals in the PSF subtracted image assure us that the close blend did not influence the position measurements for the fast star.

The different positions of the star and the nebula extrapolated to 1670 argue against a connection of the high

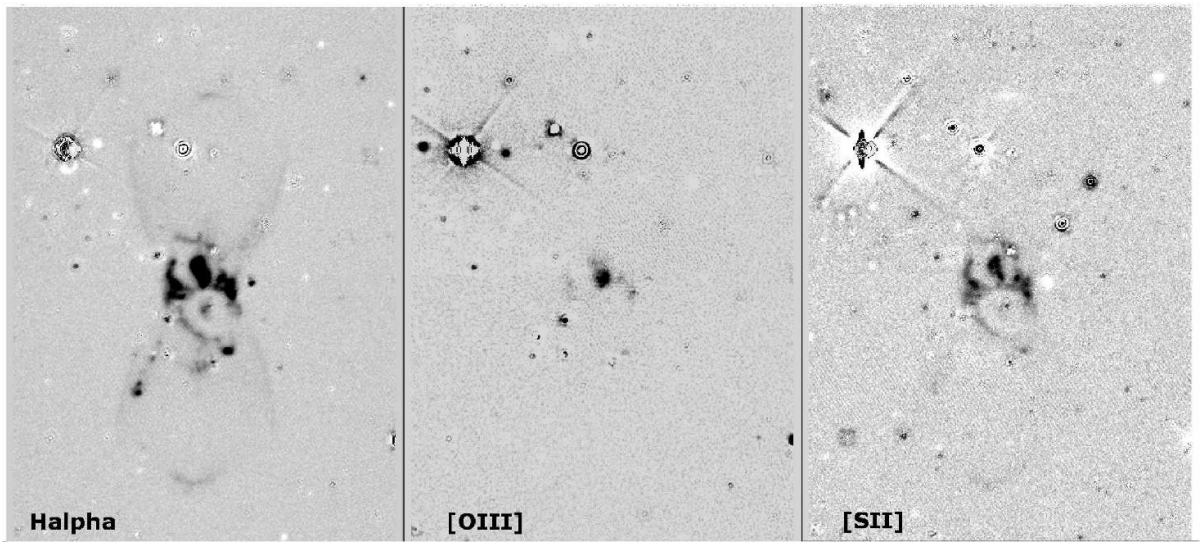

Figure 6. Gemini continuum subtracted Hα, [O III] and [S II] images. Each image is about 70×100 arcsec. North is at the top, East to the left.

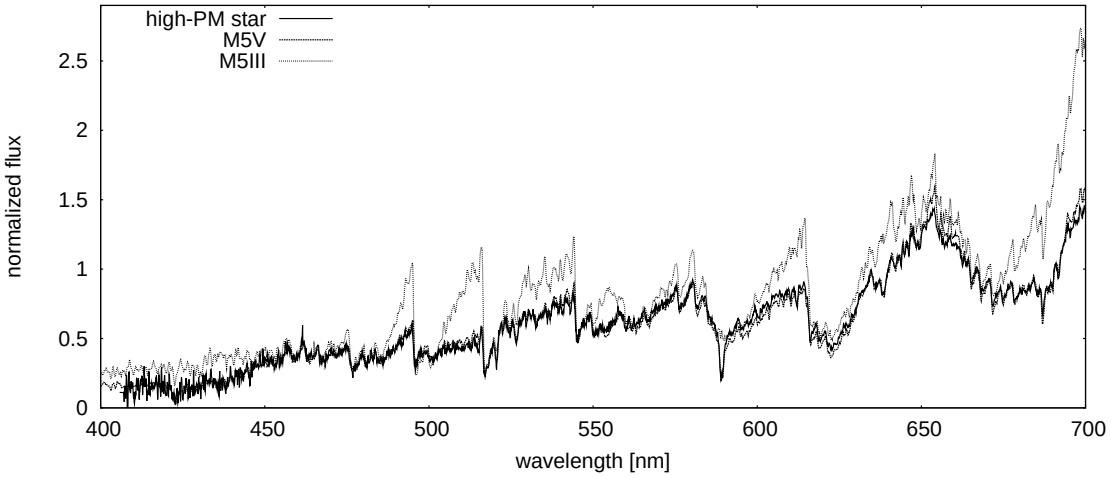

Figure 9. Spectrum of the high proper-motion star near CK Vul. Spectra of M5V and M5III type stars are plotted for comparison. The spectra were matched in intensity.

proper motion star with CK Vul. However, we do not find the positional measurements decisive. The proper motion of the nebula may be affected by different seeing, sampling or/and brightness changes of the nebula between 1991 and 2010. The possible link of CK Vul and the fast star is investigated again on the basis of photometric and spectroscopic observations of the star and the nebula in the following subsection.

4.2 Photometry and spectroscopy of the fast star

The spectrum of the fast star is presented in Figure 9. It is compared to an M5 type dwarf and giant spectra, taken from Jacoby et al. (1984). The fast star resembles a dwarf rather than a giant. It does not show either TiO absorptions as deep as a giant, or the Hα absorption. The sodium D doublet, strong in the observed star, is likely of stellar origin. The CaH1 spectral index of 0.84 (Gizis 1997) indicates that the star is not a subdwarf.

The observed brightness of the high proper motion star is $R \approx 18.5$ magnitude. Stellar type and extinction were fitted to minimalize the discrepancy between the synthetic and observed $g-r, r-i$ and $i-z$ colors (Covey et al. 2007). The best fit was obtained for an M4 type with no additional extinction. The distance of an M4 star with the apparent $r = 18.85$ is (240 ± 40) pc, derived from the color-luminosity relation (Jurić et al. 2008). If we used the M5 type, derived from the spectroscopy, the distance would shrink to (140 ± 40) pc.

The spectrum of the high proper-motion star in Figure 9 was not corrected for interstellar extinction. The comparison with the spectrum of the unreddened M dwarf taken from Jacoby's library demonstrates that the fast star is not reddened, contrary to CK Vul. Both the distance and the interstellar reddening indicate, that the fast star is a fore-

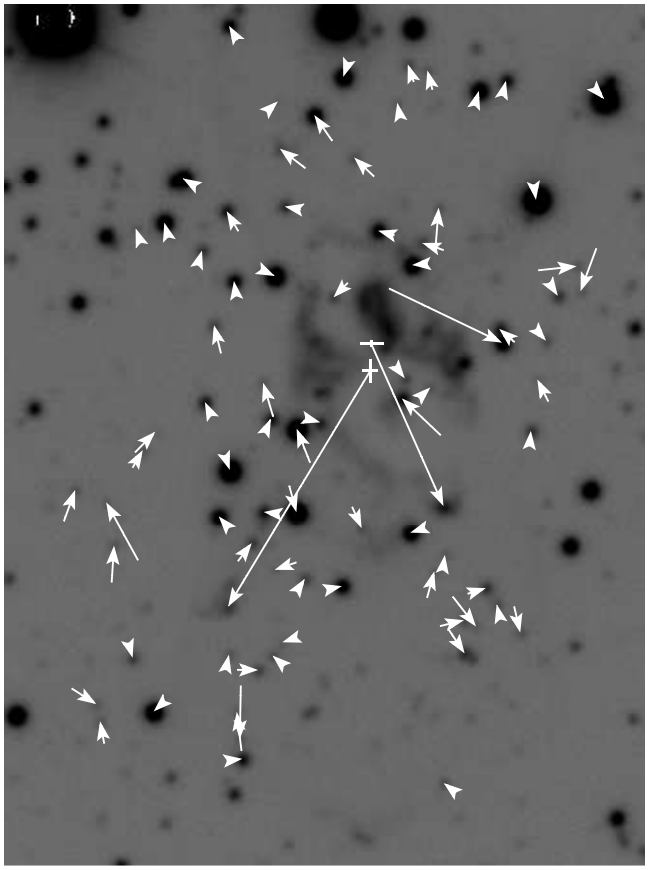

Figure 8. The Gemini Hα image of the field of CK Vul. The proper motions represented by arrows derived from the 1991 and 2010 images are exaggerated by a factor of 17.9, corresponding to the movement since 1670. A logarithmic flux scale is used. North is at the top, East to the left. The image scale is 66×47 arcsec.

ground star, located much closer than CK Vul. The tangential velocity of the star is 330 km/s for the distance of 140 pc. The heliocentric radial velocity of the star is $-50\,\mathrm{km\,s^{-1}}$.

The kinematical properties of the fast star are not consistent with the galactic disk. Such deviations are frequently observed in the solar neighbourhood for non-metal-poor dwarfs. Lépine et al. (2003) discuss possible mechanisms explaining those deviations.

5 VARIABLE STARS

5.1 Brightness evolution of the variable stars

Two stars located within $3-4$ arcsec of the expansion centre in the plane of the sky show pronounced variability (Figure 7). The apparent separation of the two variable stars is about 2 arcsec.

The comparison of the brightness of the field stars between 2010 and 1991 is presented in Figure 10. The $g'r'i'z'$ photometry was transformed to R magnitudes for the 2010 Gemini image (Smith et al. 2002). Two of the field stars showing significant brightness changes and the high proper motion star are marked with a different symbol.

The lightcurves of the two variable stars between 1991 and 2010 are shown in Figures 11 and 12. One of the variable stars (referred to as the 2nd variable) became significantly fainter during the observing period, while the other one (1st variable) has brightened. Shara et al. (1985) considered the latter star as a central star candidate and estimated its brightness as $R = 20.7 \pm 0.5$ in August 1983.

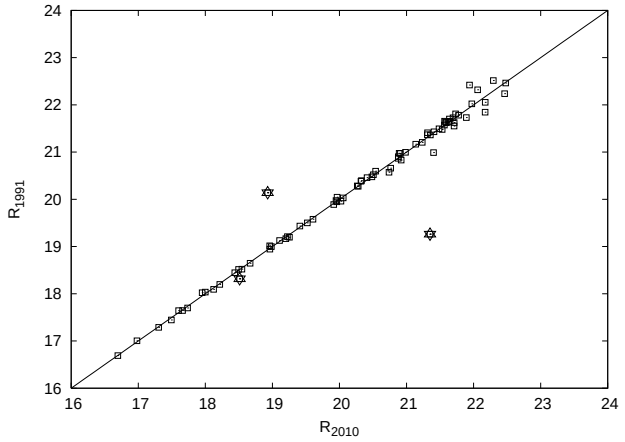

Figure 10. Comparison between 2010 June 23 and 1991 August 10 R band magnitudes of stars in the field of CK Vul. Three stars in the vicinity of the expansion centre, characterized with high proper motion or magnitude change are marked.

The observed decline of the 2nd variable continues for at least 20 years, and the increase of the brightness of the 1st variable for 30 years. We were able to measure the colour change for the 1st variable using the IPHAS 2005 and GMOS 2010 $r'i'$ observations. The $r'-i'$ index of variable 1 was equal to 1.73 in 2005 and to 1.61 in 2010 (in the Vega system), thus it changed by $\Delta(r'-i') = -0.12 \pm 0.08$ during 5 years. The r' magnitude decreased by 0.20 ± 0.05 magnitude. For dust characterized by $R_V = 3.1$, the brightness change between 1991 and 2005 of $\Delta r' = 0.2$ would imply a change of the index $\Delta(r'-i')$ of -0.05 (Cardelli et al. 1989). The observed colour change of $\Delta(r'-i') = -0.12$ suggest low value of the R_V, although this requires further confirmation.

Observed photometric indicies of the 1st variable are best fitted with the synthetic colors of a K4 main sequence star and $A_V = 4.4$ or an M0 star with $A_V = 3.3$. Stellar type later than M0 can be ruled out, though earlier type than K4 is possible. The 2nd variable is best fitted with a K4 star and $A_V = 3.7$. The distances to variable 1 obtained using the photometric parallax method (Jurić et al. 2008) are (540 ± 100) pc for a K4 star and $A_{r'} = 3.7$ and (440 ± 80) pc for an M0 star and extinction of $A_{r'} = 2.8$. The calculated distance to variable 2 is (2000 ± 400) pc, assuming extinction of $A_{r'} = 3.1$.

The obtained extinction and spectral types must be treated with caution. We assumed the variables to be main sequence stars and the Galactic extinction law with $R_V = 3.1$.

5.2 Spectra of the variable stars

The spectra of both variables are presented in Figures 13 and 14. The spectrum of variable 1 has much better quality than that of variable 2, due to difference in brightness of both stars. No stellar lines are identified in the spectrum

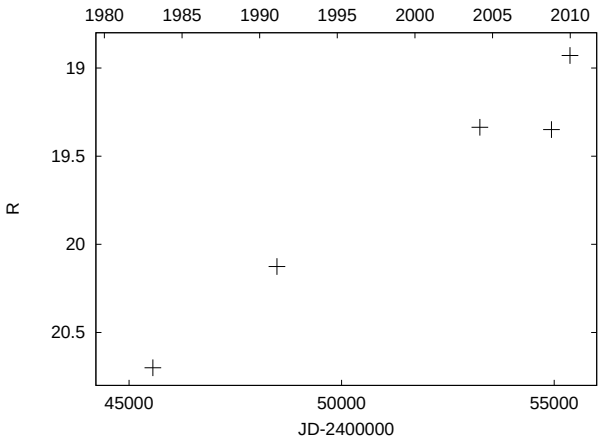

Figure 11. Evolution of the R band brightness of the 1st variable star in the field of CK Vul. The sloan r' observations have been transformed to Johnson R.

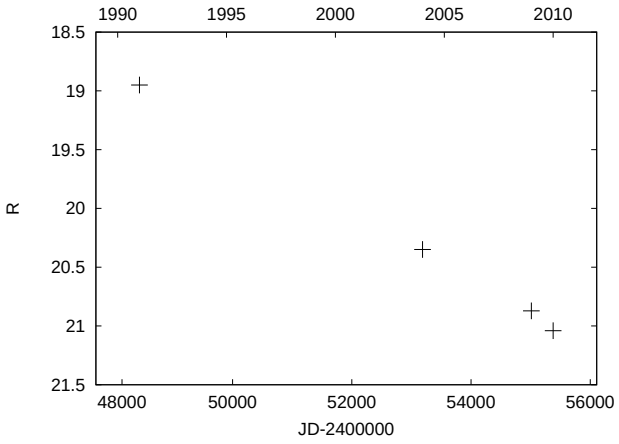

Figure 12. Evolution of the R band brightness of the 2nd variable star in the field of CK Vul. The sloan r' observation have been transformed to Johnson R.

of variable 1, apart from the Hα absorption (which is difficult to confirm because of the superposition of the star and blob 6) and the stellar contribution to the Na I 5890 and 5896Å absorption. Variable 1 was reported to show Hα absorption by Naylor et al. (1992), although their spectrum had worse quality from that ours.

Neither spectrum shows molecular bands. An M0 or later type star can be ruled out on the basis of the shape of the stellar continuum. In order to match the spectrum of variable 1 to a spectrum of a K4V star, we need to apply the reddening of $A_V \approx 5.7$ - much higher than from photometric observations ($A_V = 4.4$). This may arise from uncertain calibration of the spectroscopic observations (see section 3.3).

We detected a saturated Na I 5890 and 5896Å doublet of interstellar origin (with a possible contribution of the stellar absorption) in both spectra (Figure 13). In addition, several diffuse interstellar bands (DIB) are superimposed on the continuum of the 2nd variable. The strongest one, with an equivalent width (EW) of 2 Å, is the 6284 Å feature. Other fainter DIBs are present at 5781, 5798 and 6613 Å. Those features are not detectable in the spectrum of variable 2 due to the poor S/N ratio.

A strong (EW $\approx$ 1 Å) absorption is seen at 6705 Å in the spectrum of variable 1. It is also present (and possibly stronger) in the spectrum of variable 2. We identify this feature as a resonance Li I line.

A stellar origin of the 6705 Å line is doubtful. Lithium is depleted in low mass stars before they reach the main sequence phase, so the two stars would have to be very young to show strong 6705 Å absorption. We do not find any evidence that the two stars reside in a star forming region or an open cluster. The two stars appear to lie at different distances along the line of sight. The EW of the Li I line of 1Å would require one of the highest lithium overabundances observed in stars (Soderblom et al. 1993).

An alternative identification for the absorption line could be a Ce II transition (Reyniers et al. 2002), observed in atmospheres of post AGB-stars. None of the variables appears to be an evolved star. No other stellar lines or molecular bands are detected in the spectra, while the 6705 Å line is very strong.

An interstellar origin of this line is also unlikely. Only very weak Li I absorption is observed in the sightline towards a handful of stars, e.g. ζ Oph (Howarth et al. 2002).

The variable extinction and the Li I line most likely originate in the same medium in the sightline towards the two stars. The stars could be partly obscured by the matter ejected in the 1670 explosion, similar to the blue component in V838 Mon (Tylenda et al. 2011). That produced a prominent absorption of Li I and other elements in the spectrum of V838 Mon. It is doubtful, however, that the stars are physically associated with CK Vul. The distance to variable 2 appears to be much larger than that of CK Vul, thus it is likely a background star. Variable 1 is close to the distance to CK Vul. Within uncertainties, it can be a located behind CK Vul.

5.3 Dusty cloud ejected by CK Vul

Although the two variable stars are identyfied as background objects, their spectra and photometry can be used to investigate the properties of the cloud of gas and dust ejected by CK Vul. The cloud must extend at least $\sim$ 200 AU in the direction to the expansion centre (assuming that the cloud was ejected in 1670), since both stars remain variable for at least 20 to 30 years.

In order to determine the extinction caused by the cloud, we have to disentangle it from the interstellar extinction. The interstellar medium forms two extinction layers towards CK Vul: the first one at a distance of 500 pc and the other one at 2 kpc. An object located between the two layers would be reddened by $E(B-V) \simeq 0.8$ and behind the second layer by $E(B-V) \simeq 1.25$ (Weight et al. 2003). The distance to CK Vul of 0.70 kpc indicates that the object lies between the two extinction layers observed in its direction. Most, if not all, of the reddening suffered by the nebula of CK Vul is of interstellar origin.

The lower limit for the extinction for variable 2 is $A_R = 2$, assuming that the star was not obscured by the cloud in 1990, when the first observation was made. This would require higher extinction than observed in the V band and

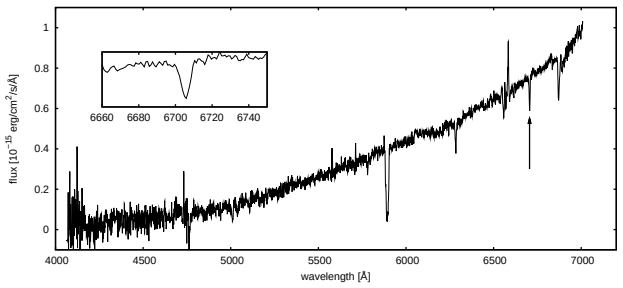

Figure 13. Spectrum of variable 1. An arrow marks the 6705 Å line. An inset presents vicinity of the 6705 Å line.

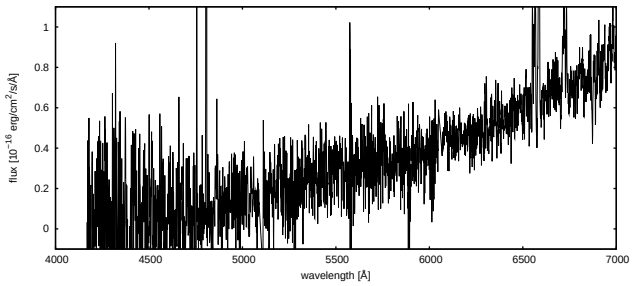

Figure 14. Spectrum of variable 2.

may be due to uncertainty in the stellar type determination or/and unusual dust properties.

If the same cloud is responsible for the variability of both stars, then its extent is at least 1650 AU (corresponding to separation of the stars of 2.2 arcsec at the distance of CK Vul). The observed EW of the line of 1 Å corresponds to a neutral lithium column density of $5 \times 10^{12}\,\mathrm{cm}^{-2}$.

Assuming the extent of the cloud is of the order of the projected distance of the two stars, the total lithium mass is of the order of $2 \times 10^{-11}\mathrm{M}_{\odot}$. The derived velocity of the cloud is about $100\,\mathrm{km\,s}^{-1}$, if it expands in a plane of the sky.

The dusty clump may be identified with the cold component seen in the SED of CK Vul (Evans et al. 2002), while the hotter component may be associated with the hotter dust obscuring the central star. The total mass of the dusty clump may be equal to $2 \times 10^{-2}\mathrm{M}_{\odot}$, previously attributed to the bipolar nebula (Hajduk et al. 2007).

6 DISCUSSION

Discussion of the nature of CK Vul, which continues since its re-discovery by Shara & Moffat (1982), is impeded by observational difficulties and apparent lack of objects of similar characteristics. The central source was detected only in the radio domain and appears to remain (partially?) obscured. Its temperature and luminosity are high enough to balance the recombination of O^+ in its vicinity. The geometry of the obscuring body is unknown (Hajduk et al. 2007). We can only very roughly constraint the central source luminosity and temperature. The luminosity of a few solar luminosities and a temperature of 60 000 K would result in a very small diameter of the emitting body (less than 1000 km). However, in the case of much higher luminosity the source would be able to ionize all the nebula or, if obscured, would be much more luminous source in the infrared.

An accreting white dwarf is heated to a temperature of 10-20kK. A thermonuclear runaway will heat the white dwarf but this is short-lasting as only the surface is heated - after the runaway, the star goes back to its previous temperatures. Using equations of Townsley & Gänsicke (2009), a temperature of 60kK corresponds to an accretion rate of $10^{-8}\,\mathrm{M}_{\odot}\,\mathrm{yr}^{-1}$. At this $\dot{\mathrm{M}}$, the luminosity of the white dwarf is about $0.5\,\mathrm{L}_{\odot}$. (It depends on the mass of the white dwarf). The thermal time scale (the rate over which the star cools down if the accretion stops) is 200 yr (for an $0.9\,\mathrm{M}_{\odot}$ white dwarf). So if the thermonuclear runaway in 1670 AD ended a phase of such high accretion, the current parameters are not implausible. Or the accretion may still continue at this rate. MV Lyr is a known CV with parameters similar to this.

The remnants of the object may be enhanced in Li. The velocities of the ejected envelope range from tens to almost $1000\,\mathrm{km\,s}^{-1}$, comprising both symmetric and nonsymmetric components. A massive cloud of dust and gas was ejected.

The model of a light nova can qualitatively reproduce the lightcurve of CK Vul (Hajduk et al. 2007; Miller Bertolami et al. 2011). In the nova scenario, the lithium could have been produced during the outburst of CK Vul (D'Antona & Ventura 2010). However, the nova scenario cannot account for other properties of CK Vul. The infrared SED of CK Vul shows two maxima corresponding to dust shells of 550 K and 25 K (Evans et al. 2002), which are hard to explain in the framework of the nova explosion. The nova scenario is also at odds with the large mass and the observed range of velocities of the expelled material.

The total energy radiated by CK Vul during its outburst of about 10^{47} erg, places this object close to NGC 3432 OT2008-9 on the energy-time diagram for observed transients (Soker & Kashi 2011). Soker & Kashi (2011) propose that outbursts of intermediate luminosity optical transients may be powered by mass accretion onto a main-sequence companion. It can explain the expansion velocity of the fastest parts of the CK Vul nebula (of the order of the escape velocity from a MS star), though most of the matter was expelled with lower velocities. The small radius of the ionizing source is at odds with this scenario. The white dwarf would not cool as fast as in CK Vul, unless the outburst occured on the surface of the star.

Kato (2003) proposed a merger scenario. Such a scenario can reproduce the variety of light curves and the amplitude of the outburst (Tylenda & Soker 2006). One of the merger components should have been lithium rich to explain the lithium enhancement of the remnants (e.g. a planet, young star or an RGB/AGB star). The temperature of the source in the expansion centre suggests that one of the objects was or had become a white dwarf after the outburst. Again, the outburst would have to occur on the surface of the star and not affect the deeper layers.

The born-again scenario (Evans et al. 2002) would be in line with the observed lithium overabundance. However, the lack of hydrogen-deficient material in the nebula does not agree with the evolutionary models for VLTP. Neither the diffuse induced nova nor VLTP events can account for the very low luminosity of CK Vul only 340 yr after the outburst (Miller Bertolami et al. 2011).

ACKNOWLEDGMENTS

The research reported in this paper has partly been supported by a grant No. NN203 403939 financed by the Polish Ministery of Sciences and Higher Education. PvH acknowledges support from the Belgian Science Policy office through the PRODEX program. Based on observations obtained at the Gemini Observatory, which is operated by the Association of Universities for Research in Astronomy, Inc., under a cooperative agreement with the NSF on behalf of the Gemini partnership: the National Science Foundation (United States), the Science and Technology Facilities Council (United Kingdom), the National Research Council (Canada), CONICYT (Chile), the Australian Research Council (Australia), Ministério da Ciência, Tecnologia e Inovação (Brazil) and Ministerio de Ciencia, Tecnología e Innovación Productiva (Argentina). The William Herschel Telescope and its service programme are operated on the island of La Palma by the Isaac Newton Group in the Spanish Observatorio del Roque de los Muchachos of the Instituto de Astrofsica de Canarias. This paper makes use of data obtained from the Isaac Newton Group Archive which is maintained as part of the CASU Astronomical Data Centre at the Institute of Astronomy, Cambridge.

REFERENCES

Alard C., Lupton R. H., 1998, ApJ, 503, 325
Cardelli J. A., Clayton G. C., Mathis J. S., 1989, ApJ, 345, 245
Covey K. R., et al., 2007, AJ, 134, 2398
D'Antona F., Ventura P., 2010, Proc. IAU Symp., 268, ed. C. Charbonnel, et al., 395
Drew J., et al., 2005, MNRAS, 362, 753
Evans A., van Loon J. Th., Zijlstra A. A., Pollacco D., Smalley B., Tyne V. H., Eyres S. P. S., 2002, MNRAS, 332, 35
Fukugita M., Ichikawa T., Gunn J. E., Doi M., Shimasaku K., 1995, AJ, 1996, 111, 1748
Gizis J. E., 1997, AJ, 113, 806
Hajduk M., et al., 2007, MNRAS, 378, 1298
Harrison T. E., 1996, PASP, 108, 1112
Howarth I. D., Price R. J., Crawford, I. A., Hawkins, I., 2002, MNRAS, 335, 267
Jacoby G. H., Hunter D. A., Christian C. A., ApJSS, 56, 257
Jurić M., et al., 2008, ApJ, 673, 864
Kato T., 2003, A&A, 399, 695
Lépine S., Rich R. M., Shara M. M., 2003, AJ, 125, 1598
Miller Bertolami M. M., Althaus L. G., Olano C., Jiménez N., 2011, MNRAS, 415, 1396
Nahar S. N., Pradhan A. K., 1997, ApJS, 111, 339
Naylor T., Charles P. A., Mukai K., Evans A., 1992, MNRAS, 258, 449
Reyniers M., Van Winckel H., Biémont E., Quinet P., 2002, A&A, 395, 35
Shara M. M., Moffat A. A., 1982, ApJ, 258, 41
Shara M. M., Moffat A. A., Webbink R. F., 1985, ApJ, 294, 271
Smith J. A., et al., 2002, AJ, 123, 2121
Soderblom D. R., Jones B. F., Balachandran S., Stauffer J. R., Duncan D. K., Fedele S. B., Hudon J. D., 1993, AJ, 106, 1059
Soker N., Kashi A., 2011, arXiv:1107.3454
Steffen W., Koning N., Wenger S., Morisset C., Magnor M., 2010, arXiv:1003.2012
Townsley, D. M., Gänsicke, B. T., 2009, ApJ, 693, 1007
Tylenda R., Soker N., 2006, A&A, 451, 223
Tylenda R., Kamiński T., Schmidt M., Kurtev R., Tomov T., 2011, A&A, 532, 138
Weight A., Evans A., Albinson J. S., Krautter J., 1993, A&A, 268, 294